

# AN INFLUENCE OF PHYSICAL ELECTRODE MODELS IN RAT'S HEAD FORWARD MODELLING

**David Kuřátko**

Doctoral Degree Programme (1), FEEC BUT

E-mail: xkurat01@stud.feec.vutbr.cz

Supervised by: Zbyněk Raida

E-mail: raida@feec.vutbr.cz

**Abstract:** Reliable inverse imaging of source currents in rat's brain requires moderate models of fields to calibrate inverse solvers. The article is focused on the comparison of measured potentials on rat's brain surface with and without physical electrode models. For the simulation purpose, the 3D models of the brain, the cerebrospinal fluid, and the skull were developed from magnetic resonance images (MRI). Moreover, the pink noise was added to measured potentials to obtain more realistic results. Simulations showed higher values of potentials when physical electrode models were considered. Fortunately, the presence of electrode models does not influence the potential waveform. Therefore, the inclusion of electrode models to forward modelling can contribute to the increase of accuracy of an inverse solver, and thus the localization of current sources in rat's brain.

**Keywords:** Forward model, rat's head, electrodes

## 1 INTRODUCTION

Brain waves can be measured on rat's head surface as electrical potentials [1]. The localization of brain wave sources requires a forward modelling and an inverse solver [2]. The forward model is aimed to calculate the potentials at the surface electrodes from known source parameters. Solution of the forward problem is then organized into the so-called lead-field matrix, which is essential for solving the inverse problem. The equation of the forward model is then given by:

$$\mathbf{X} = \mathbf{L}\mathbf{S} + n \quad (1)$$

where  $\mathbf{X}$  is the vector of simulated potentials (lead-field matrix) on the brain surface,  $\mathbf{S}$  corresponds to the current density vector,  $\mathbf{L}$  denotes the transfer matrix determined by the head volume conductor (3D model), and  $n$  represents noise.

The inverse solver is asked to localize wave sources in the brain from the lead-field matrix based on forward modelling. The localization can be described mathematically by the following equation:

$$\mathbf{O}(\mathbf{S}) = \min \|\mathbf{X} - \mathbf{L}\mathbf{S}\|^2 \quad (2)$$

In this paper, only the electro-quasi-static formulation of Maxwell equations and a single brain model was used. Comparison of different formulations (static, quasi-static, and full-wave) and various meshes differing in the density, the type and the geometrical accuracy can be found in [4].

## 2 ELECTROMAGNETIC MODELS AND SIMULATION SETUP

### 2.1 3D MODELS

The brain model was based on the magnetic resonance imaging (MRI), the skull one on the computed tomography images (CT), and the cerebrospinal fluid was created manually.

Creation of the 3D model was based on the segmentation of relevant areas in medical images (MRI, CT). The segmentation marked areas in three slices (axial, coronal, and sagittal) by an automatic algorithm (Region growing), where several seeds were placed manually in relevant areas. Then, the algorithm selected surrounded points with similar properties based on the MRI. Increasing iterations, the algorithm selected other area points to have the relevant area approximately selected. The algorithm cannot select anatomical parts with different properties, for instance ventricles. Within that case, a manual selection across all three slices has to be performed. Fig. 1 shows the segmentation of the brain MRI; the red colour represents chosen areas.

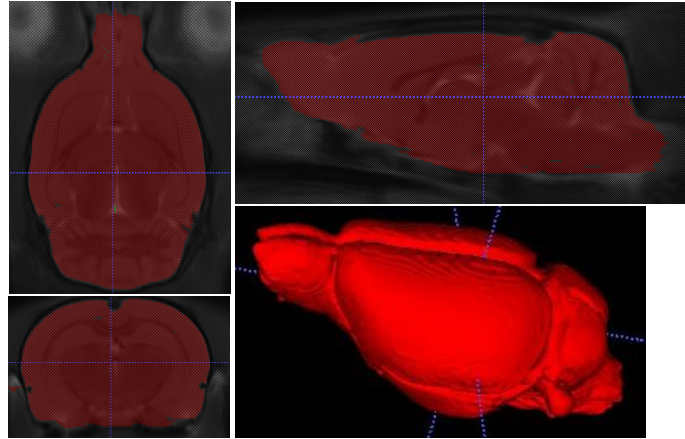


**Figure 1:** Segmentation of MRI in slices: axial (top left), coronal (bottom left), sagittal (top right), and corresponding 3D brain model (bottom right).

When creating the model by a segmentation procedure, several mesh errors can be caused. These errors are originated from the volume approximation between slices. Therefore, all the models have to be consequently processed with Blender, MeshLab, Autodesk MeshMixer, and Autodesk Fusion 360. After removing duplicated surfaces and edges of elements, correcting unevenness, protrusions and sharp edges and modifying the orientation of mesh elements, a new mesh was generated to preserve anatomy of the models. Finally, the brain model was resized to the length  $l = 27$  mm, the width  $w = 15$  mm and the height  $h = 10$  mm which are the approximate dimensions of the brain of an adult Wistar rat.

In Fig. 2, the composite model of the head is shown in the vertical cut crossing the head centre. The model consists of the brain, the fluid and the skull converted into voxels with the edge length  $l_e = 0.7$  mm. The bottom picture in Fig. 2 proves that all the models are properly aligned thanks to the conversion to voxels.

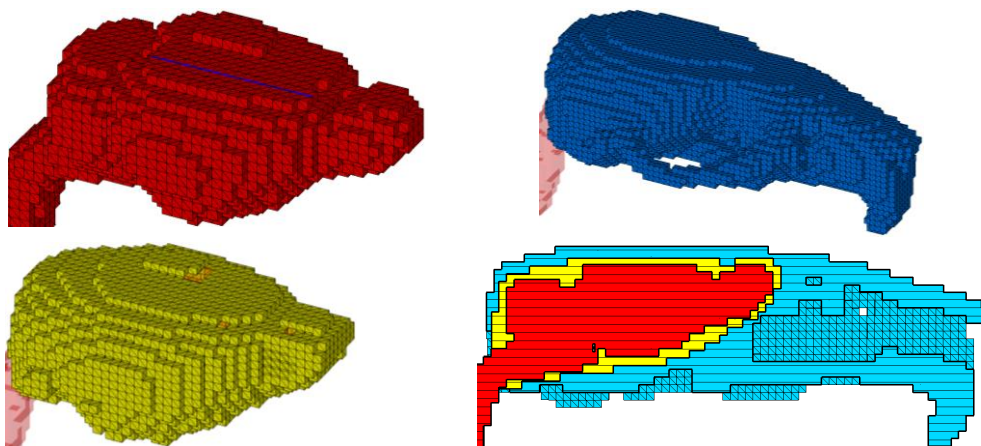


**Figure 2:** Voxel models: the brain (top left), the cerebrospinal fluid (bottom left), the skull (top right), vertical cut crossing the center of the composite model (bottom right).

For simulation purposes, the brain model was embedded into the cerebrospinal fluid and the skull. The brain model and the skull model come from different Wistar rats. Therefore, the brain was scaled in proportion for the best fitting of the cavity volume in the skull. The free space among the brain and the skull was filled in by the cerebrospinal fluid. After that, the brain model, the cerebrospinal fluid and the skull were converted to voxels. Thanks to the conversion, the brain, the fluid and the skull can be aligned (potential gaps are eliminated), and simulations are accelerated.

## 2.2 SIMULATION SETUP

The composite model was imported to the CST Studio Suite 2018 to evaluate the spatial distribution of computed quantities. For this reason, the electro-quasi-static formulation of Maxwell equations was used. The formulation neglects displacement currents and time derivatives of the magnetic flux density in Faraday's law. Brain waves are represented by the spatial distribution of the electric potential or the electric field intensity. The quasi-static model is evaluated by the low frequency domain solver of the EM Studio. The LF solver calculates following equation:

$$\nabla \cdot [(j\omega\epsilon + \sigma)\nabla\varphi] = \nabla \cdot \mathbf{J}_s \quad (3a)$$

Here,  $\epsilon$  denotes permittivity,  $\varphi$  corresponds to electric potential,  $\mathbf{J}_s$  is primary or impressed current,  $\sigma$  represents electric conductivity, and  $\omega$  denotes angular frequency.

The brain can be understood as a volumetric source of a current produced by populations of neurons. Various frequencies of electromagnetic waves can be observed due to the complex behaviour of the brain. Generally, many studies on neural oscillations concluded that deeper parts of the brain excite electromagnetic waves with rather lower frequencies and the frequency raises in the evolutionary younger areas closer to the brain surface [3]. However, appropriate mapping of frequencies is still not available due to the complexity and inter-individual variability of the brain.

Brain waves propagate at frequencies from  $f_{min} = 0.1$  Hz to  $f_{max} = 100$  Hz [2]. However, the power of the electroencephalograph (EEG) signal decreases with the increasing frequency by the factor of  $1/f$  [1]. Thus, the brain was decided to be simulated at the alfa frequency 10 Hz which corresponds to the known peak in the spectral power of a human EEG.

Electrical parameters of tissues (the brain, the cerebrospinal fluid and the skull) were approximated by corresponding parameters of human tissues. The relative permittivity was  $\epsilon_r = 4.07 \cdot 10^7$  [-] [6] for the brain,  $\epsilon_r = 1.09 \cdot 10^2$  [-] [6] for the cerebrospinal fluid, and  $\epsilon_r = 5.51 \cdot 10^4$  [-] [6] for the skull. On the other hands, the electric conductivity was  $\sigma = 0.33$  S/m [2] for the brain,  $\sigma = 1.79$  S/m [2] for the cerebrospinal fluid, and  $\sigma = 0.0174$  S/m [2] for the skull.

The EEG can be measured by surface electrodes when a large group of neurons is simultaneously active. This group of active neurons can be modelled as a current dipole [2]. The dipole produces electrical field propagating to the surface of rat's head where the potential can be measured by an electrode. In this paper, the dipole of the length  $l_d = 0.7$  mm and the width  $w_d = 0.1$  mm was used. This length of the dipole corresponds to the length of the element edge.

Neurons are aimed to process and transmit signals by a secreting neurotransmitter. There are two kinds of neurotransmitters [2]:

- The first one lets the signal to proliferate, and the molecules cause an influx of positive ions. The potential between intra- and extracellular environment increases to -40 mV. The potential change is called the excitatory postsynaptic potential (EPSP).
- The second one causes an outflow of positive ions which decreases the potential between intra- and extracellular environment. The potential change is called the inhibitory postsynaptic potential (IPSP) [2].

Due to the above-given reasons, the dipole in performed simulations was determined to excite the postsynaptic potential with value -60 mV.

The simulated measuring electrodes correspond to the system, which is used for real EEG recording with rats. The system consists of twelve active electrodes implanted into the surface of the cortex in homologous frontal, parietal and temporal regions of the right and left hemispheres [5]. The coordinates of active electrodes were calculated from the bregma, and their positions are obvious from the left picture in Fig. 3, whereas the right picture shows the positions of electrodes on the real rat after surgery. The ground electrode was implanted to the occipital region which is the bottom part of the brain close to the cerebellum. For simulation purposes, the rectangular shape of electrodes was used instead of the cylindrical one due to hard meshing of curved shapes by tetrahedron elements. The width of electrode was  $w_e = 0.15$  mm, the length of electrodes equal to  $l_e = 3$  mm, and material parameters corresponded to floating perfect electric conductor (PEC). The bottom part of electrodes was aligned to the brain, and this is the plane, where potentials were measured.

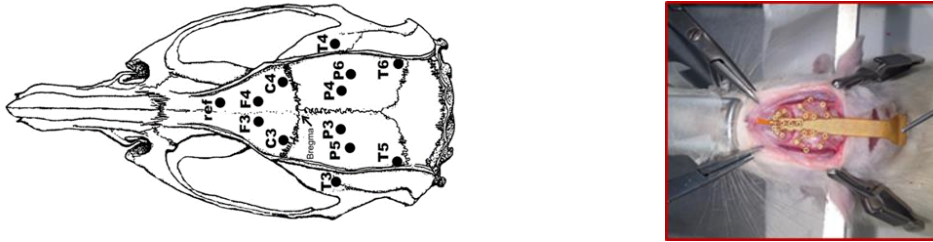


**Figure 3:** Position of active electrodes: schematic (left), real rat after surgery (right).

### 3 RESULTS

In the electro-quasi-static simulation is consistent in time, only one value of potential is available for individual electrode. From Eq. 1 is obvious that, the forward model is also defined with noise. A commonly used noise is the pink one. Therefore, the original consistent value of the potential was used to create 500 temporal samples denoted by  $n$  of the original value. After that, the pink noise was generated and added to the samples. For better clarity, only two signals measured on electrodes F3 and T6 are shown. These signals were chosen due to the highest distance between the electrodes. In Fig. 4, the comparison of measured potentials for the electrode F3 (left) and T6 (right) with the physical model of scanning electrodes and without the electrode models are depicted. Obviously, the same pink noise was added to all four signals. Comparison of results shows that the simulation with physical electrode models provides a higher level of the potential for both the electrodes (F3, T6).

In Fig. 5, the electric potential depending on the measuring trajectory  $p_1$  is shown. The measuring trajectory  $p_1$  is the line on the top of the brain surface (see blue line in the top left picture in Fig. 2). Obviously, the electrodes do not affect the potential waveform on rat's brain surface. On the other hand, the simulation with physical electrode models provides results with a higher potential along the whole measuring trajectory  $p_1$ . The right picture in Fig. 5 proves the distribution of electric field intensity near active electrodes on rat's brain surface. Influence on the rest of models is obvious (the cerebrospinal fluid and the skull).

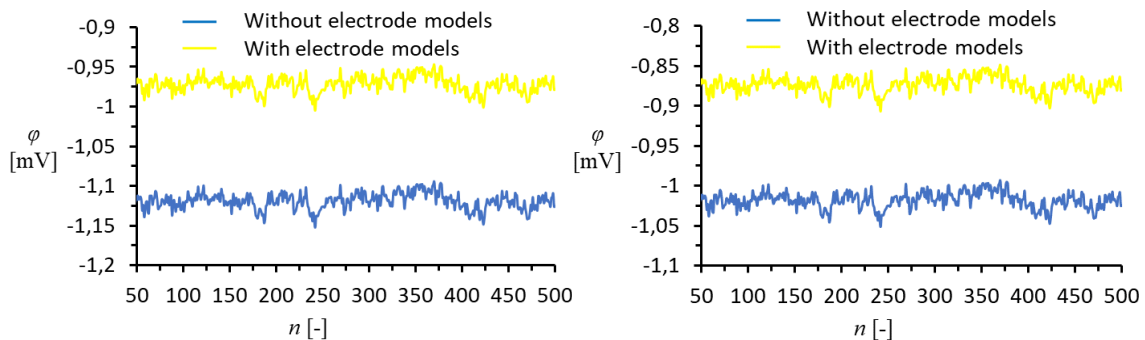


**Figure 4:** Comparison of measured potentials with and without physical electrode models for: electrode F3 (left), electrode T6 (right).

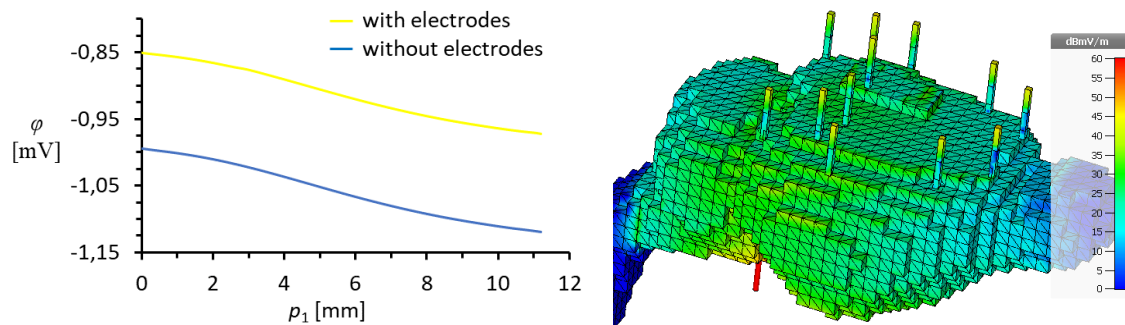


**Figure 5:** Electric potential depending on the coordinate of the measuring trajectory  $p_1$  for simulation with and without electrode models (left), distribution of electric field intensity near electrodes (right).

## 4 CONCLUSION

In the paper, the presence of the physical electrode models in the rat's head forward modelling was described. For simulation, the composite head model was developed and proceeded by the CST software. The simulated model consisted of the brain, the cerebrospinal fluid, and the skull. The simulation was based on the electro-quasi-static approach. The excitation dipole corresponded to the post-synaptic potential of the neuron. Comparison of the simulation with and without physical electrode models showed that the presence of electrode models produced a dependency differing in the magnitude, but not in the shape of waveform. These results can be directly used for current localization in real rats: consistent potentials on electrodes represent columns in the lead-field matrix and a different position of the excitation source corresponds to rows. In near future, the whole realistic electrode system will be examined, wherever the new electrode with the specific excitation signal will be added to represent the brain stimulation.

## ACKNOWLEDGEMENT

The presented work was supported by the Czech Science Foundation under the grant no. 18-16218S, and Internal Grant Agency of Brno University of Technology project no. FEKT-S-17-4713. Simulations were performed in the SIX Research Centre thanks to the support of the National Sustainability Program, the grant no. LO1401.

## REFERENCES

- [1] HE, B. Neural engineering. 1<sup>st</sup> ed., rev. New York (U.S.): Kluwer Academic/Plenum, 2005. ISBN: 978-0-306-48609-8.
- [2] HALLEZ, H., VANRUMSTE, B., GRECH, R., et all. Review of solving the forward problem in EEG source analysis. *Journal of NeuroEngineering and Rehabilitation*, 2007, vol. 4, no. 1, DOI: 10.1186/1743-0003-4-46
- [3] NUNEZ, P. L., SRINIVASAN, R. Electric fields of the brain: the neurophysics of EEG, 2<sup>nd</sup> ed. rev. New York (U.S): Oxford University Press, 2006. ISBN: 9780195050387
- [4] KURATKO, D., RAIDÁ, Z., CUPAL, M., et. all, Electromagnetic modelling of rat's brain: comparison of models and solvers, *Proceedings of International Workshop on Computing, Electromagnetics, and Machine Intelligence (CEMi 2018)*. Stellenbosch (South Africa), 2018.
- [5] PÁLENÍČEK, T., FUJÁKOVÁ, M., BRUNOVSKÝ, M. et. all. Electroencephalographic spectral and coherence analysis of ketamine in rats: correlation with behavioural effects and pharmacokinetics. *Neuropsychobiology*, 2011, vol. 63, no. 4, DOI: 10.1159/000321803
- [6] Dielectric Properties of Body Tissues, <http://niremf.ifac.cnr.it/tissprop>, last accessed 2019/03/25